Characterization of high density lipoprotein subspecies: structural studies by single vertical spin ultracentrifugation and immunoaffinity chromatography

Marian C. Cheung,* Jere P. Segrest,[1,]†† John J. Albers,*,† John T. Cone,** Christie G. Brouillette,** B. Hong Chung,** Moti Kashyap,*** M. Alice Glasscock,** and G. M. Anantharamaiah****

Departments of Medicine* and Pathology,† School of Medicine, Harborview Medical Center, University of Washington, Seattle, WA 98104; Departments of Pathology,** Biochemistry,†† and Medicine,†† and the Atherosclerosis Research Unit,** University of Alabama at Birmingham Medical Center, Birmingham, AL 35294; and Department of Medicine,*** University of Cincinnati Medical Center, Cincinnati, OH 45267

Abstract Affinity columns containing anti-apolipoprotein A-I or A-II were used to fractionate plasma into subpopulations of lipoprotein particles containing: *a*) apoA-I [Lp(A-I)], *b*) apoA-I and A-II [Lp(A-I with A-II)], and *c*) apoA-I but no A-II [Lp(A-I without A-II)]. Single vertical spin and electron microscopy analyses of these HDL subpopulations demonstrated that acid elution from the affinity columns caused no detectable change in size and density of the three subpopulation particles. Analysis by nondenaturing gradient gel electrophoresis of the three subpopulations found in four normal subjects identified nine HDL subspecies, designated [1] through [9] in order of increasing size; [3–7] were the major subspecies. Lp(A-I with A-II) is composed primarily of subspecies [3],[5], and [6], and may contain some subspecies [2] and [7], while Lp(A-I without A-II) represents mainly [4] and [7] and the minor subspecies [1],[2],[8], and [9]. HDL subspecies [4],[5], and [6] are found in the standard sequential flotation density cuts for both HDL_3 and HDL_2, which illustrates the limitations of the latter terminology. Using single vertical spin ultracentrifugation, HDL fractions were located and isolated for physical and chemical analyses, including immunoassay for apoA-I, A-II, and C-II. The distribution of the Lp(A-I without A-II) particles corresponded closely to the apoC-II distribution. An apoA-I-rich, cholesteryl ester- and phospholipid-poor subspecies was identified in the dense HDL fractions. HDL subspecies [7] was found to contain at least three separate subspecies designated [7a], [7b], and [7c]. Based on these and previously published results (Brouillette, C. G., et al. 1984. *Biochemistry.* **23:** 359–367), we propose that the HDL subspecies adjacent in size generally differ by the association/lack of association of a hinge-like domain of amphipathic helixes in a single molecule of apoA-I.—**Cheung, M. C., J. P. Segrest, J. J. Albers, J. T. Cone, C. G. Brouillette, B. H. Chung, M. Kashyap, M. A. Glasscock, and G. M. Anantharamaiah.** Characterization of high density lipoprotein subspecies: structural studies by single vertical spin ultracentrifugation and immunoaffinity chromatography. *J. Lipid Res.* 1987. **28:** 913–929.

Supplementary key words gradient gel electrophoresis • electron microscopy

High density lipoproteins (HDL) are operationally defined as lipoproteins within the density range of 1.063 to 1.21 g/ml that possess α-electrophoretic mobility. The apolipoproteins (apo) that have been identified in HDL are apoA-I, A-II, A-IV, B, C-I, C-II, C-III, D, E, and F. By using immunochemical techniques, Kostner and Alaupovic (1) demonstrated that not all apolipoproteins are found on the same HDL particles. More recently, HDL particles containing various combinations of the different apolipoproteins have been isolated (2, 3).

The heterogeneous nature of human HDL (d 1.063 to 1.210 g/ml) with respect to size and density is well documented (4). Zonal ultracentrifugation has been used to isolate HDL subspecies designated HDL_1 (d 1.080–1.090 g/ml) (5), HDL_2 (d 1.063–1.125 g/ml) (6, 7) and HDL_3 (d 1.125–1.21 g/ml (6). Sequential isopycnic ultracentrifugation has been used to separate HDL_2 and HDL_3 (8). Analytical ultracentrifugation has been used to measure levels of HDL_2 and HDL_3 as well as to elucidate the existence of other subspecies of HDL (9). The HDL subspecies HDL_3 and HDL_2 have also been shown to be heterogeneous (4, 6, 10). Finally, HDL subspecies have been shown to have differing metabolic roles (11).

Detailed studies of apolipoprotein compositional heterogeneity have been hampered by the lack of suitable

---

Abbreviations: HDL, high density lipoproteins; SVS, single vertical spin; VAP, vertical autoprofile; Lp(A-I), lipoproteins containing apoA-I; Lp(A-I with A-II), lipoproteins containing apoA-I and apoA-II; Lp(A-I without A-II), lipoproteins containing apoA-I without apoA-II.

[1]To whom all correspondence should be addressed at Atherosclerosis Research Unit, University of Alabama at Birmingham Medical Center, Birmingham, AL 35294.

methodology for isolation and quantitation of even those HDL subspecies that differ only in size and density. Ultracentrifugation methodology that has been used for isolation of the different HDL subspecies (5–8) suffers particularly from extended centrifugation times (36 hr to almost 1 week) that lead to as yet incompletely characterized changes in the structural and compositional integrity of the isolated subspecies.

In view of the importance of the apolipoprotein components of an HDL particle in determining its functional role and metabolic fate, we have begun to isolate HDL particles with distinct apolipoprotein compositions using antibodies specific for each apolipoprotein (12). We found that apoA-I immunoaffinity chromatography removed virtually all HDL from plasma, indicating that most HDL particles contain apoA-I. On the contrary, apoA-II immunoaffinity chromatography removed only certain HDL density fractions from plasma. The present study reports the characterization of HDL subspecies using a combination of apoA-I and A-II immunoaffinity chromatography with single vertical spin (SVS) ultracentrifugation and negative stain electron microscopy. Ultracentrifugation by the SVS procedure has the advantage of short spin times (90–150 min) and thus less particle degradation than sequential flotation (13–15). Using this combination of techniques, we have identified in this study a minimum of eleven distinct subspecies of HDL.

MATERIALS AND METHODS

Vertical autoprofile analyses

The vertical rotor procedure (vertical autoprofile, VAP) used for the analysis of HDL subspecies was a modification of one described earlier for single spin separation and analysis of the major classes of lipoproteins (13–15). The gradient was formed in 5-ml Beckman Quik-Seal tubes (Beckman Spinco Division, Palo Alto, CA, cat. no. 34212) as follows: 1.4 ml of plasma was adjusted to density 1.21 g/ml and overlayered with 3.5 ml of a d 1.06 g/ml KBr solution. The tubes were then placed in a Beckman VTi 80 vertical rotor and spun at 80,000 g until $\omega^2 t = 3.50 \times 10^{11}$ (ca. 90 min).

The tubes were punctured and the effluent was analyzed by a continuous flow cholesterol monitor developed in our laboratory (14). The basic system that allows computer sampling of the data has been described elsewhere (15).

HDL-VAP difference plots

The HDL-VAP difference plots were constructed from the raw data used to generate the normal HDL-VAP plots in the following manner. Several features that are a consequence of the nature of the VAP itself required special consideration when constructing the difference. First, the time between consecutive points on the curve is variable both within a run and from run to run. Consequently, the time scale for the occurrence of points for the subtracted curve was normalized to that of the first curve. When more than one subtraction was to be done on an individual plasma, the same time scale was used for all subtractions. A linear interpolation algorithm was used to calculate the heights that the points in the second curve would have at the times corresponding to the first curve.

Second, due to the necessity of routine pump tubing changes as well as other factors, the time between puncturing the tube and curve-start can vary slightly. As a consequence of this, the curve-start was taken as zero time for both curves. Implicit in this is the assumption that some cholesterol-containing material is always at the bottom of the tube.

A third consideration is that the absolute area under the curve of the same sample can vary from one rotor to the next, principally because of the necessity of changing tubing and reagent. As a consequence, the heights of all of the curves must be corrected to take into account the difference in absolute area of the control. This was done by multiplying the uncorrected heights by the ratio of the area of the reference curve in the first rotor to the area of the reference curve in the second rotor. After these changes were made on each set of curves, the differences were calculated using a point subtraction, taking into account changes in dilution between the samples when necessary.

Preparation of anti-A-I and anti-A-II immunosorbent

Antisera to apoA-I and A-II were obtained from goats and rabbits as described (16). Antibodies specific to either apoA-I or A-II were isolated from the respective antisera by affinity chromatography using HDL covalently coupled to CNBr-activated Sepharose 4B (12). The antibodies used in this study were previously documented to be specific for either A-I or A-II by Ouchterlony gel diffusion as well as immunoprecipitation (12). Affinity-isolated antibodies to apoA-I and A-II were covalently coupled to CNBr-activated Sepharose 4B at a ratio of 5–8 mg/ml of gel, according to the procedure provided by Pharmacia (Pharmacia Fine Chemicals, Piscataway, NJ). These antibody–Sepharose gels are stable for months when stored in the presence of 0.02% Merthiolate at 4°C.

Subjects

Blood samples in this study were obtained from six healthy normolipidemic adults with normal-to-high HDL cholesterol levels (three men and three women) after a 12–14 hr overnight fast. Venous blood was drawn into Vacutainer tubes (Becton-Dickinson, Rutherford, NJ) containing disodium EDTA (1.5 mg/dl). On separation of

plasma by low-speed (1000 *g*) centrifugation at 4°C, 0.5 g/l sodium azide, 0.01 g/l chloramphenicol, and 0.0005 g/l gentamycin were promptly added. The plasma was immediately used for isolation of lipoproteins by immunoaffinity chromatography and/or vertical rotor centrifugation.

Isolation of lipoproteins by immunoaffinity chromatography

Lipoproteins containing A-I [Lp(A-I)]. Fresh plasma was incubated with anti-A-I immunosorbent for 1 hr at 4°C. Proteins that did not bind to the immunosorbent were washed off with 0.01 M Tris, 0.15 M NaCl, 1 mM EDTA, pH 7.4, and concentrated under vacuum to a volume equal to or less than the starting plasma volume to test for presence of apoA-I and A-II by specific immunoassays (16, 17). Nonspecifically bound proteins were removed by washing the gel with 0.1 M $NaHCO_3$, 0.5 M NaCl, 1 mM EDTA, pH 8.0, followed by 0.1 M sodium acetate, 0.5 M NaCl, 1 mM EDTA, pH 4.0. ApoA-I-containing lipoproteins bound to the immunosorbent were eluted with 0.1 M acetic acid, 1 mM EDTA, pH 3.0. The lipoproteins eluted were immediately buffered to physiological pH with solid Tris, dialyzed against 0.15 M NaCl, 1 mM EDTA, pH 7.4, and concentrated under vacuum for vertical rotor centrifugation and other analyses.

Lipoproteins containing A-I and A-II [Lp(A-I with A-II)]. Fresh plasma was incubated with anti-A-II-immunosorbent and processed as described above.

Lipoproteins containing A-I without A-II [Lp(A-I without A-II)]. ApoA-II–free plasma (the nonbinding plasma proteins from the anti-A-II affinity column) [P(– A-II] was incubated with anti-A-I immunosorbent for 1 hr at 4°C. Again, nonbinding proteins, nonspecifically bound proteins, and apoA-I-containing lipoproteins (without apoA-II) were sequentially washed from the immunosorbent and processed as previously described.

Electron miscroscopy

HDL subspecies fractions were stained with 2% (w/v) potassium phosphotungstate, pH 5.9, and examined with a Philips EM 400 microscope on carbon-coated Formvar grids.

Nondenaturing gradient polyacrylamide gel electrophoresis

The molecular size distribution of lipoprotein particles isolated from anti-A-I and anti-A-II immunosorbents was estimated by nondenaturing gradient polyacrylamide gel electrophoresis on Pharmacia precast PAA 4/30 gels and scanned densitometrically as described (12). Thyroglobulin, apoferritin, catalase, lactate dehydrogenase, and bovine albumin (HMW Standard, Pharmacia) were used as calibrating proteins. We used the following Stokes diameters of these calibrating proteins in our calculations: thyroglobulin, 170 Å; apoferritin, 122 Å; catalase, 104 Å; lactate dehydrogenase, 82 Å; and bovine albumin, 75 Å.

Isolation of HDL subspecies

For most of the HDL subspecies isolation studies, a rapid (2.5 hr) single vertical spin (SVS) procedure was used to isolate HDL subspecies fractions. Plasma samples (3.5 ml), adjusted to d 1.18 g/ml with KBr, were overlayered with 13.5 ml of KBr solution at d 1.12 g/ml and subjected to a 2.5-hr ultracentrifugation in a TV-865B rotor at 65,000 RPM on a Beckman L8-80 or a Sorvall OTD-2 ultracentrifuge at 10°C. The tubes were fractionated by downward flow using a Hoeffer gradient fractionator and a Technicon or Pharmacia proportioning pump.

For one of the isolation studies, a 5.5-hr SVS procedure was used to isolate HDL subspecies fractions. This procedure represents the HDL-VAP gradient conditions applied to a larger rotor. Plasma samples were adjusted to d 1.21 g/ml with KBr and 5 ml was overlayered with 12 ml of a d 1.06 g/ml KBr solution. This gradient was spun at 65,000 rpm for 5.5 hr at 10°C in a TV865B Sorvall rotor and fractionated as described above. The collected fractions were analyzed for apolipoproteins and lipid.

Chemical analyses

Albumin determination was done by the method of Doumas, Watson, and Biggs (18). Total protein determinations were performed using the method of Lowry et al. (19). Apolipoprotein and LCAT mass analyses were done by radioimmunoassay procedures (13, 20–22) or radial immunodiffusion assays (16, 17). Phospholipid analyses were done by the method of Steward (23). Unesterified cholesterol and cholesteryl ester were measured by enzymatic methods using either a Boehringer-Mannheim kit (Boehringer-Mannheim Diagnostics, Indianapolis, IN) or an ABA-200 AutoAnalyzer (Abbott Laboratories). Triacylglycerides were measured enzymatically using a Boehringer–Mannheim kit by the method of Bocolo and David (24).

RESULTS

Analysis of HDL subspecies by HDL-VAP

The gradient formed during the vertical rotor ultracentrifugation method used for HDL-VAP analysis is shown in **Fig. 1A.** The recorder output of the cholesterol monitor for a typical HDL-VAP is shown in Fig. 1B. The peak at the right represents the sum of the plasma LDL and VLDL. When these two fractions are subtracted out mathematically, the dashed curve is generated. It is important to realize that the species are not at equilibrium with the gradient after a spin of only 90 min. As a consequence, estimates of the density of a subspecies based on its flotation characteristics in the gradient will, in general, overestimate that density. This is particularly true for the less dense HDL fractions. Because the top density is 1.073 g/ml, it is reasonable to expect that all the LDL and VLDL will have floated to the top, and this was con-

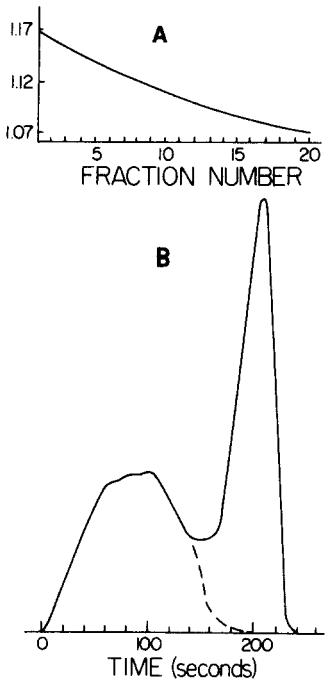

Fig. 1. Key features of HDL-VAP analysis. A, Final density gradient obtained after single vertical spin ultracentrifugation using 1.4 ml of 1.21 g/ml density-adjusted plasma overlayered with 3.5 ml of a 1.06 g/ml KBr solution and spun at 80,000 *g* for approx. 90 min ($\omega^2 t = 3.50 \times 10^{11}$) in a VTi80 rotor. The y-axis is in units of g/ml. B, Typical HDL-VAP output of the continuous-flow cholesterol monitor. The dotted line represents the adjusted curve after computer subtraction of LDL and VLDL contained in the sample.

sistently observed. Individuals high in Lp(a) (a lipoprotein class with an average d 1.07 g/ml) have a shoulder on the left-hand side of the HDL-VLDL peak.

Immunoaffinity chromatography

Plasma from four of the six normolipidemic subjects studied, two male (M-1 and M-2) and two female (F-1 and F-2), were subjected to immunoaffinity chromatography. **Table 1** gives the plasma cholesterol and triglyceride levels of all six subjects. Three lipoprotein fractions were isolated, designated Lp(A-I), Lp(A-I with A-II) and Lp(A-I without A-II) using the immunoaffinity chromatography scheme diagrammed in **Fig. 2.** Because apolipoprotein A-II was always quantitatively bound and eluted with apoA-I by the A-I affinity column, plasma without A-I [P(– A-I)]contains neither A-I nor A-II and thus is identical to plasma without A-I and A-II [(P(– A-I – A-II)]. Every particle bound and eluted from the A-II affinity column was presumed to contain A-I as well as A-II.

Fig. 3A shows HDL-VAP analyses of the two nonbinding plasma lipoprotein fractions, P(– A-I) and P(– A-II), compared to the starting plasma, for subject F-2 (see Figs. 6 and 7). HDL from this subject was chosen for detailed presentation because the subject had the highest total HDL of the four subjects studied by immunoaffinity chromatography and thus displayed the most clearly defined HDL-VAP analysis. The following conclusions (valid for all four subjects) can be made. *a*) At best, only minor subspecies missing apolipoprotein A-I exist in the HDL density region. *b*) The HDL fractions entirely without apolipoprotein A-II from all four subjects, when examined by HDL-VAP, have a major peak in the lower density half and a minor peak in the higher density half of the profile.

Fig. 3B–D are HDL-VAP analyses of the three HDL fractions, Lp(A-I), Lp(A-I with A-II), and Lp(A-I without A-II). In contrast to Fig. 3A, the right-hand peak, representing particles in the LDL and VLDL density regions that presumably contain A-I and/or A-II, has been mathematically removed. This was done because very minor peaks consistently appear in this position. The results are in agreement with Fig. 3A; that is, in subject F-2, Lp(A-I) resembles whole HDL, Lp(A-I with A-II) is composed

TABLE 1. Plasma lipid concentrations

Plasma Lipids	Subjects					
	M-1	M-2	M-3	F-1	F-2	F-3
	mg/dl					
Cholesterol	230	161	120	169	166	162
Triglyceride	78	64	17	79	82	47
HDL cholesterol	69	59	63	63	84	58

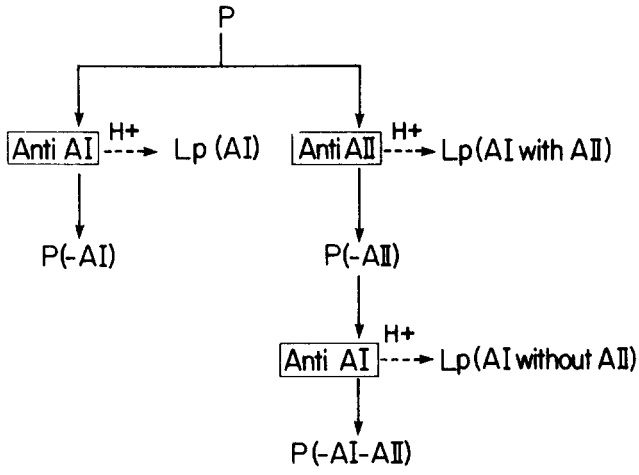

Fig. 2. Flow diagram for immunoaffinity column chromatography preparation of HDL subspecies containing apoA-I and/or A-II. The boxes represent affinity columns containing monospecific antibody directed against the apolipoprotein indicated. P, starting whole plasma; P(– A-I), plasma from which all particles containing apoA-I have been removed; P – A-II), plasma from which all particles containing apoA-II have been removed; P(– A-I – A-II), plasma from which all particles containing apoA-I and A-II have been removed; Lp(A-I), lipoprotein particles eluted from an anti-A-I column; Lp(A-I with A-II), lipoprotein particles eluted from an anti-A-II column; Lp(A-I without A-II), lipoprotein particles, from which apoA-II particles have been previously removed, eluted from an anti-A-I column.

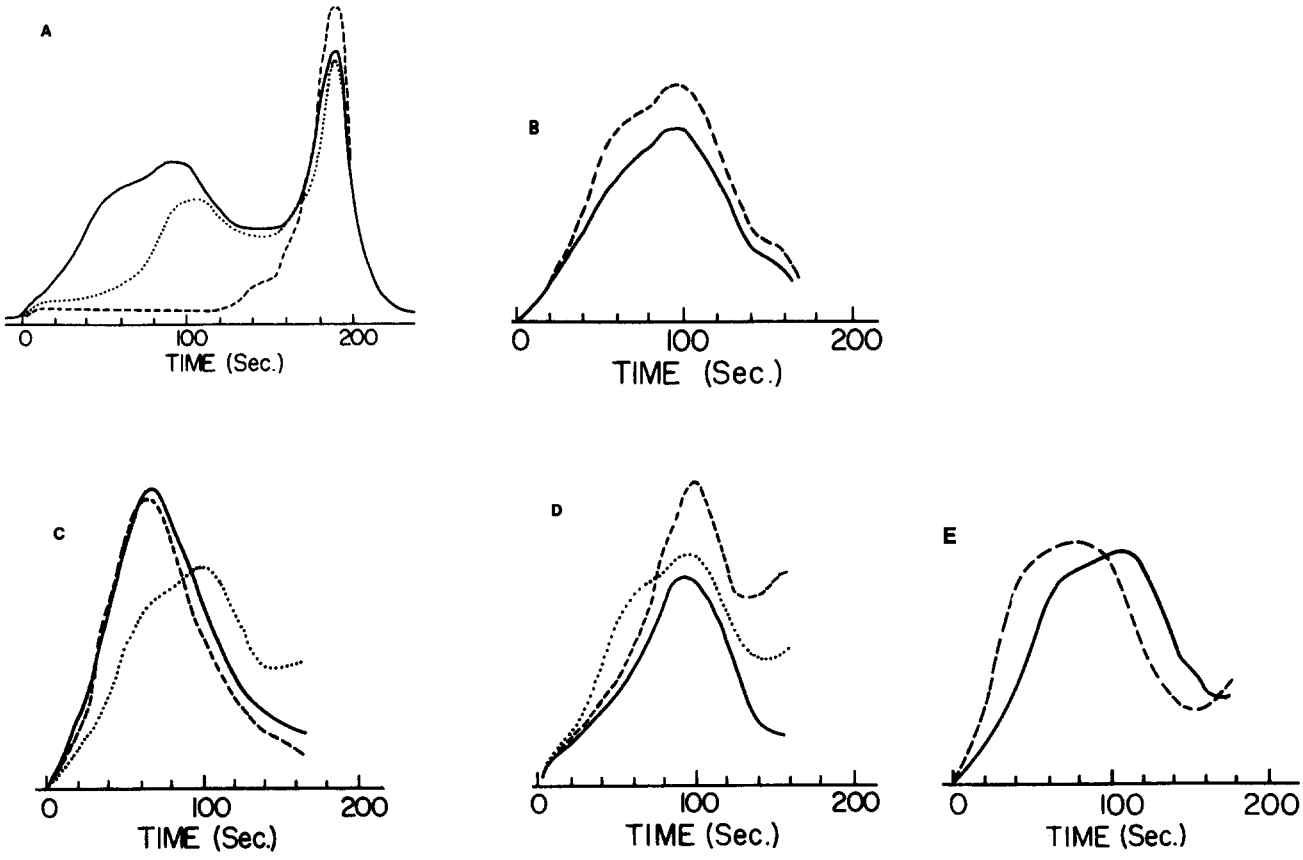

Fig. 3. HDL-VAP analyses of plasma and lipoprotein particles from subject F-2 with HDL cholesterol level of 84 mg/dl. A, Whole plasma (P) (—); plasma with A-I removed, P(– A-I) (----); plasma with A-II removed, P(– A-II), (••••). B, ApoA-I-containing lipoprotein particles, Lp(A-I) (—) versus difference plot of starting plasma minus P(– A-I) (----). C, Lipoprotein particles containing both A-I and A-II, Lp(A-I with A-II) (—) versus difference plot of starting plasma minus P(– A-II) (----) versus whole plasma (••••). D, Lipoprotein particles containing A-I but no A-II, Lp(A-I without A-II) (—) versus difference plot of starting plasma minus Lp(A-I with A-II) (----) versus whole plasma (••••). Note that P – [Lp(A-I with A-II)] is not necessarily identical mathematically to Lp(A-I without A-II). E, HDL-VAP analyses of control HDL (—) and HDL modified by incubation with a synthetic peptide analog of the amphipathic helix (----).

mostly of high density HDL particles, and Lp(A-I without A-II) is composed mostly of low density HDL particles, although the latter curve appears to have a minor higher density component. Similar results were found for the other three subjects (Fig. 7 and results not shown).

We know from negative stain electron microscopy that the sizes of HDL particles are changed following incubation with synthetic peptides (data not shown). Fig. 3E shows that alteration of the size and/or density of HDL subspecies, produced by incubation with a synthetic peptide analog of the amphipathic helix (25–27), also profoundly alters the HDL-VAP profile of the HDL subspecies. Thus, if the size and/or density of Lp(A-I) particles are not altered by acid elution, then, for example, the HDL-VAP of Lp(A-I) should be essentially identical to the mathematical subtraction of P(– A-I) from the starting plasma (Fig. 3B). In the same way, the HDL-VAP of Lp(A-I with A-II) should equal P(– A-II) subtracted from the starting plasma (Fig. 3C). Because we did not perform HDL-VAP on P(– A-I – A-II), no difference plot identity, equal to the subtraction of P(– A-I–A-II) from P(–A-II), could be calculated for Lp(A-I without A-II). However, with the exception of the region beyond 140 sec, subtraction of Lp(A-I with A-II) from the starting plasma is a close approximation to Lp(A-I without A-II) (Fig. 3D). Within the limits of the procedure, the conditions of difference plot identity are met for subject F-2 (Figs. 3B–D), as well as for the other three subjects, F-1, M-1, and M-2 (data not shown), providing evidence that the three eluted HDL fractions are not significantly altered by the acid elution step.

Fig. 4 shows electron micrographs of Lp(A-I), Lp(A-I with A-II), and Lp(A-I without A-II) from subject F-2. **Fig. 5** shows histogram plots of the size distribution of

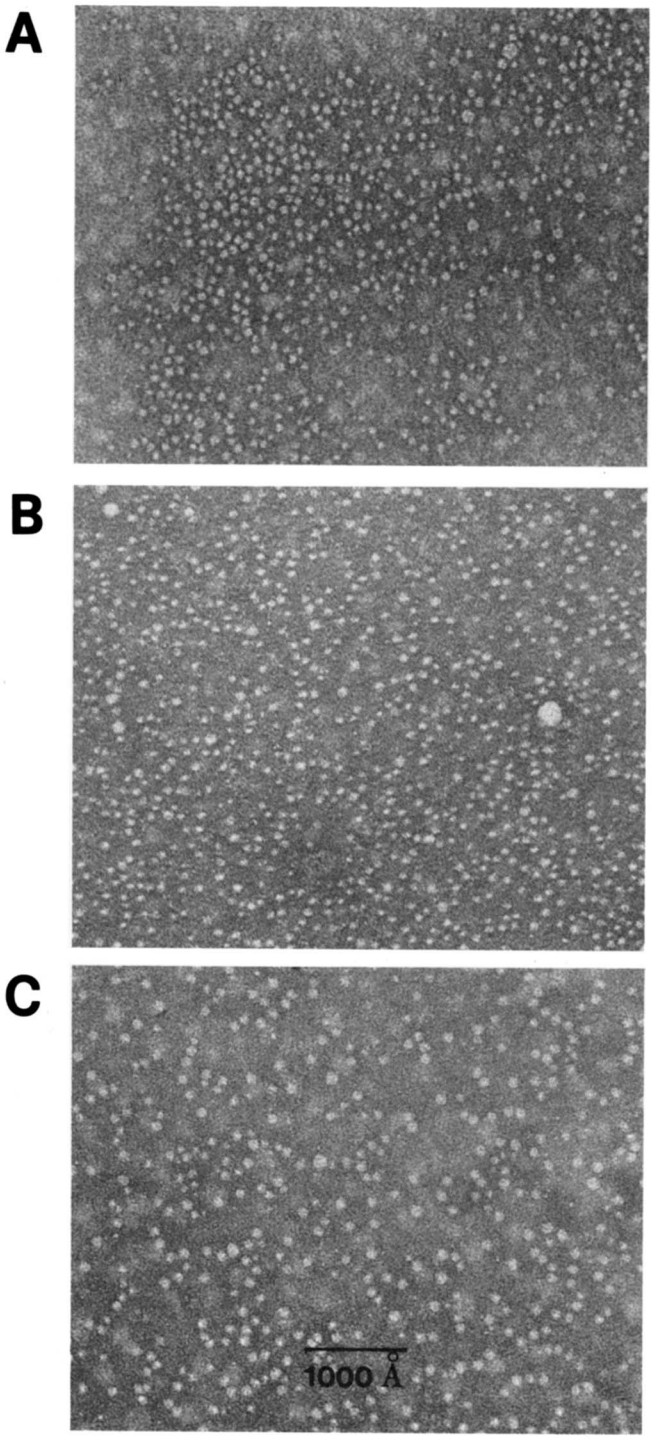

Fig. 4. Electron micrographs of the three eluted particles from subject F-2. A, Lp(A-I); B, Lp(A-I with A-II); C, Lp(A-I without A-II).

HDL particles in the three eluted HDL subpopulations, Lp(A-I), Lp(A-I with A-II) and Lp(A-I without A-II), from the four subjects. Lp(A-I with A-II) represents a smaller size fraction of the Lp(A-I) particles. There are two components to Lp(A-I without A-II), one collection of particles larger than, and a second collection of particles smaller than, the average particle size of Lp(A-I with A-II). The shape of the HDL-VAP analysis of Lp(A-I without A-II) (Figs. 3D and 7) are consistent with a bimodal particle size distribution for this fraction.

The most detailed analysis of the three eluted HDL subpopulations, Lp(A-I), Lp(A-I with A-II), and Lp(A-I without A-II), is provided by nondenaturing gradient gel electrophoresis **(Fig. 6).** We use brackets to distinguish HDL subspecies defined by nondenaturing gradient gel electrophoresis (e.g., HDL[1], HDL[7a], etc.) from HDL subspecies defined by the analytical ultracentrifuge (HDL_3, HDL_2, etc.). In our terminology, the smaller, more dense HDL subspecies have the smaller numerical designators.

To summarize the results of Fig. 6, at least nine HDL subspecies based on size alone can be distinguished; five of these subspecies, [3], [4], [5], [6], and [7], represent the majority of total HDL. In all four subjects Lp(A-I with A-II) is composed primarily of the major subspecies [3], [5], and [6] (there is also some [2] and [7]). Also, in all four subjects Lp(A-I without A-II) is composed primarily of the major subspecies [4] and [7], consistent with the bimodal nature of Lp(A-I without A-II) already noted, as well as the minor subspecies [1], [2], [8], and [9]. The mean Stokes diameters of the nine subspecies of these four subjects are shown in **Table 2.** Finally, Fig. 6 (F-1 and M-1) shows that HDL_2 and HDL_3, isolated by the standard flotation density cuts (d 1.063–1.125 and d 1.125–1.21 g/ml, respectively) (9), overlap by several gradient gel particle sizes; HDL_2 contains [7] and [6], with some [5] and [4], whereas HDL_3 contains [3], [4], and [5], with some [6]. There is also some loss of resolution of the individual subspecies following the extended centrifugation.

Apolipoprotein compositional analyses of HDL subspecies

Figs. 7A and B represent HDL-VAP analyses of whole plasma and of HDL fractions Lp(A-I with A-II) and Lp(A-I without A-II) isolated from the female subject (F-1) and the male subject (M-1), respectively. The results are qualitatively similar to those described for the male subject M-2 and the female subject F-2 (Fig. 3 and data not shown).

Plasma from subjects F-1 and M-1 were subjected to the 2.5-hr HDL-SVS procedure. Fractions were collected and analyzed for cholesterol and for apoA-II and C-II by radioimmunoassay (16, 25). The results are consistent with the conclusion reached by the immunoaffinity chromatography studies just described in that Lp(A-I with A-II) defined by the apoA-II curves in **Figs. 8A and B,** is complex and is located predominantly in the denser half of the HDL region. Subspecies [7], represented by the prominent right-hand cholesterol shoulder in Figs. 8A and 8B, is localized to the region flanking fraction 20. The

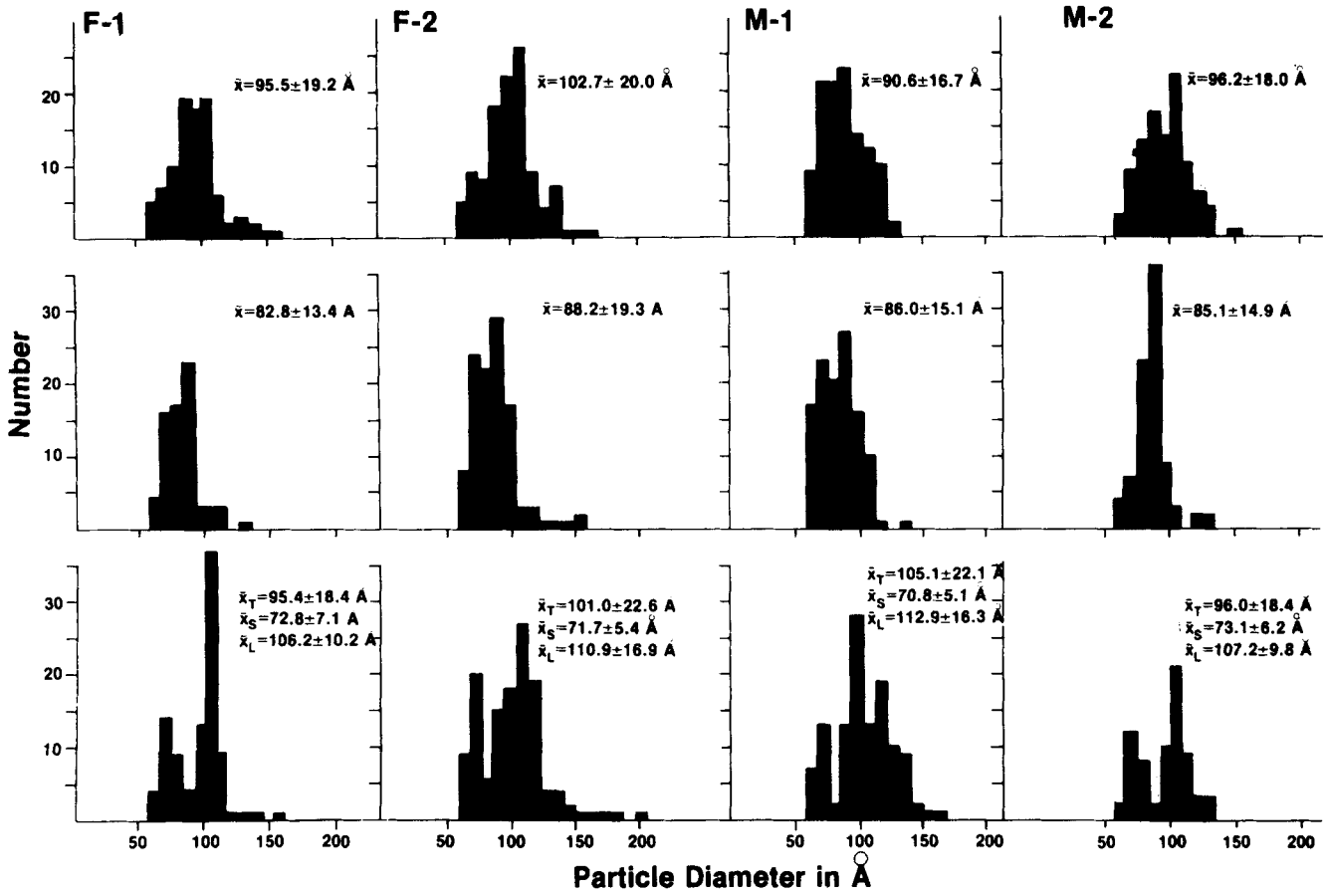

Fig. 5. Morphographic analysis of particle diameters for the three eluted particles from the four subjects studied by immunoaffinity column chromatography. Subjects F-1 and F-2 are females; M-1 and M-2 are males. For each eluted particle, n = 100. Top row, Lp(A-I); middle row, Lp(A-I with A-II); bottom row, Lp(A-I without A-II). Particle diameter means ($\bar{x}$) and standard deviations (±) are displayed on each graph. For Lp(A-I without A-II), three particle diameter means are shown: $\bar{x}_T$, total; $\bar{x}_S$, smaller mode; $\bar{x}_L$, larger mode.

apoC-II curves indicate that this is also the region of greatest C-II concentration, although other fractions also contain this protein. Further, the apoC-II and cholesterol curves show three recognizable shoulders in the HDL[7] region, indicating that subspecies [7] is partially resolvable into three fractions. These three regions in the HDL[7] peak are designated on the figures as [7a], [7b], and [7c].

A comparison of Figs. 7 and 8 indicates that the HDL-VAP curves for Lp(A-I with A-II) in Fig. 7 correspond closely to the curves for apoA-II in Fig. 8. More remarkable is the close correspondence between the HDL-VAP curves for Lp(A-I without A-II) in Fig. 7 and the curves for apoC-II in Fig. 8. The implications of this latter observation will be examined more closely in the discussion.

Isolation and analysis of HDL species

In **Fig. 9A,** the insert is an HDL-VAP analysis of plasma from a third male subject, M-3. Fig. 9A is a 2.5-hr HDL-SVS fractionation of plasma from M-3 analyzed for cholesterol. Seven pools indicated by the bars were analyzed for apolipoproteins A-II and C-II by radioimmunoassay. These pools were also subjected to gradient gel electrophoresis (Fig. 9B). Since whole plasma was fractionated, plasma protein bands contaminate all of the pools, especially pools 1 and 2. Nevertheless, it is clear from Fig. 9B that pools 5–7 contain the HDL subspecies [7]. Examination of the gradient gel analyses of pools 5 and 6 suggests the presence of at least three different-sized particles within subspecies [7] (indicated by the arrows between lanes 7 and 8). Finally, these seven pools were subjected to HDL-VAP (Fig. 9C). The HDL-VAP results are qualitatively in good agreement with the gradient gel analysis. For example, the heterogeneity of HDL subspecies [7] is illustrated by both procedures.

Detailed compositional analyses of HDL subspecies

In a final study, plasma from a third female subject, F-3, was subjected to the 5.5-hr HDL-SVS fractionation procedure. The radioimmunoassays were done in triplicate and all other chemical analyses in duplicate. **Fig. 10A** shows the results of total protein and albumin measurements for each fraction across the gradient. As expected,

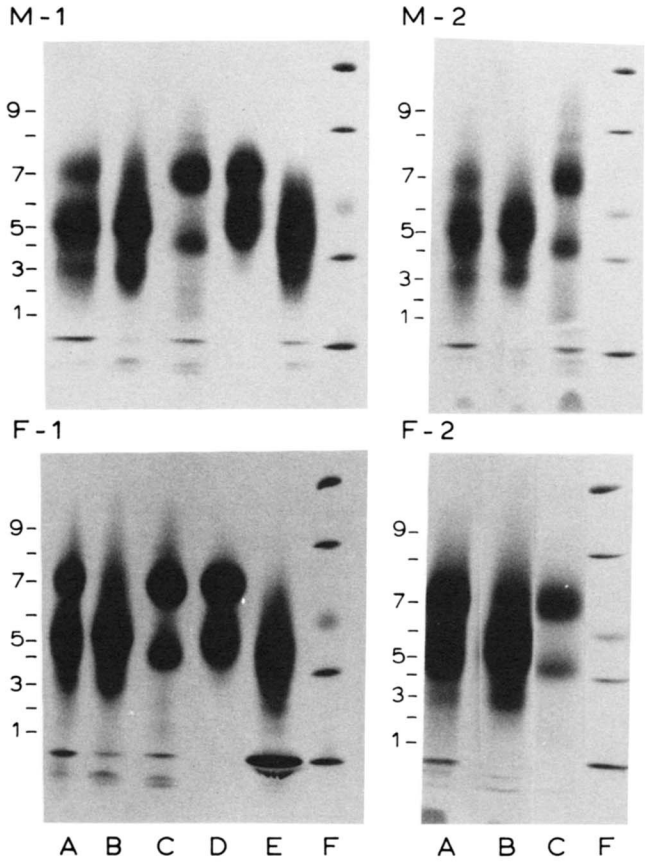

Fig. 6. Nondenaturing gradient gel electrophoresis, stained with Coomassie blue, of the three eluted particles from the four subjects studied by immunoaffinity column chromatography. The positions of subspecies 1–9 are indicated to the left of each electrophoresis for each subject. A, Lp(A-I); B, Lp(A-I with A-II); C, Lp(A-I without A-II); D, HDL_2(d = 1.063–1.125 g/ml); E, HDL_3 (d = 1.125–1.21 g/ml); F, Stokes diameter standards from top to bottom: thyroglobulin (170 Å), apoferritin (122 Å), catalase (104 Å), lactate dehydrogenase (82 Å), bovine albumin (75 Å).

most of the protein was in the bottom (left-hand) fractions. Measurable albumin was present until the fifteenth tube. The total protein analysis shows minimal fine structure in the HDL region (e.g., fractions 8 and 13).

TABLE 2. Diameter of individual HDL subspecies studied by gradient polyacrylamide gel electrophoresis

HDL Subspecies	Mean Diameter in Å
9	131.8 ± 1.1 (n = 3)
8	121.4 ± 2.0 (n = 2)
7	108.5 ± 3.8 (n = 4)
6	95.3 ± 2.5 (n = 4)
5	89.9 ± 2.4 (n = 4)
4	85.0 ± 1.2 (n = 4)
3	81.0 ± 0.9 (n = 4)
2	78.2 ± 0.8 (n = 4)
1	76.4 ± 0.8 (n = 4)

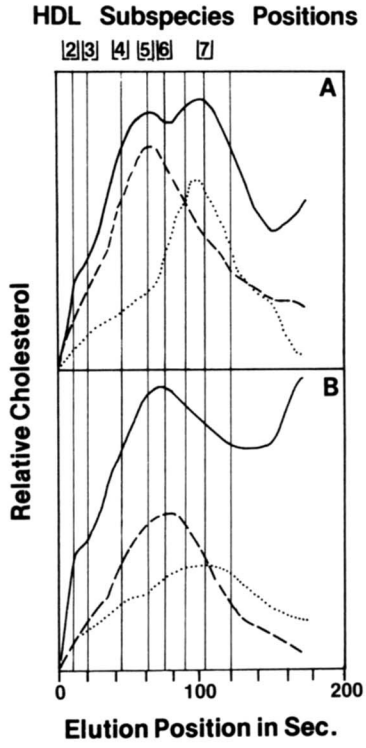

Fig. 7. HDL-VAP analyses (1.5-hr spin) of whole plasma (—), Lp(A-I with A-II) (----) and Lp(A-I without A-II) (••••) from subjects F-1(A) and M-1(B). The estimated peak centers for the HDL subspecies [2–8] are indicated.

Fig. 10B shows the results of assays for unesterified cholesterol and cholesteryl ester, as well as radioimmunoassays for apoA-I, apoA-II and apoB. The total cholesterol (cholesterol plus cholesteryl ester) curve shows well-defined peaks centered at fractions 3, 15, and 23. The latter two are broad peaks suggesting multiple components, an assumption supported by the cholesteryl ester curve, which gives some hint of subspecies within the two peaks. The radioimmunoassays show even stronger evidence for a great deal of fine structure. The apoA-I curve shows peaks or shoulders centered at fractions 3, 8, 13, 17, 21, 24, and 27. The apoA-II curve shows peaks or shoulders centered at fractions 4, 10, 13, 17, 20, and 23, corresponding closely to all but the least dense of the apoA-I peaks.

From Fig. 10B, the apoB curve remains near zero throughout the HDL regions after the first few fractions. The reason for the apparent increase in apoB in the first five fractions is unclear, particularly since bottom fractionation was used, although apoB degradation and/or the presence of Lp(a) may be involved.

Fig. 10C shows phospholipid and triacylglycerol analyses of the fractions. The phospholipid curve shows the same three peaks illustrated in the cholesterol trace with some hint of fine structure. Although triacylglycerol is found in all HDL fractions, the most obvious peak is in the bottom fractions. The origin of this peak is not clear.

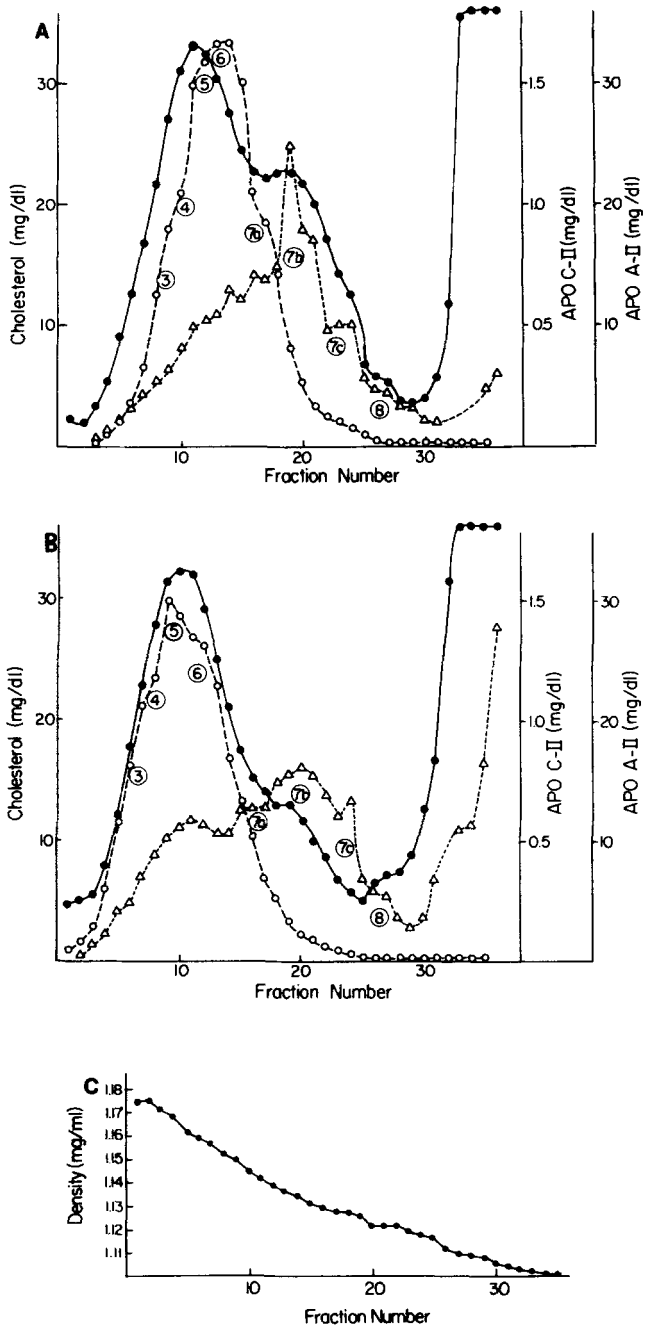

Fig. 8. HDL-SVS fractionation (2.5-hr spin) of plasma from subjects F-1 (A) and M-1 (B). (●—●), Total cholesterol measured by ABA-200; (O---O), apo A-II measured by radioimmunoassay; (△--△), apoC-II measured by radioimmunoassay. The estimated positions of HDL subspecies are indicated by the encircled numbers. C, Gradient density calibration of the 2.5-hr HDL-SVS preparative run.

The phospholipid-to-cholesteryl ester ratio shown in Fig. 10D shows an increase toward the less dense HDL subspecies, a finding opposite to that expected from simple surface-to-volume ratio considerations. This increase might be explained by postulating a progressive decrease in the apolipoprotein to phospholipid ratio in going from the more dense to less dense HDL subspecies.

Fig. 10E confirms that a progressive decrease does occur in the ratio of apoA-I and apoA-II to phospholipid in going from the more dense to the less dense HDL subspecies. This figure represents a plot of three ratios, apoA-I/phospholipid, apoA-II/phospholipid, and apoA-I/cholesteryl ester, derived from the data given in Figs. 10B and 10C. The apoA-I/phospholipid ratio reaches a minimum in the HDL[7] region. A second significant feature of the three curves in Fig. 10E is a spike in the dense HDL region between fractions 4 and 10, suggesting distinct subspecies in this region that are relatively enriched in apoA-I and apoA-II compared to *both* phospholipid and cholesteryl ester. The more dense half of this spike appears to be relatively apoA-II-poor compared to the less dense half (see Fig. 10G below).

Fig. 10F is a replot plot of total cholesterol from fractions isolated by the 5.5-hr HDL-SVS method, identical to that in Fig. 10B, and is included for comparison.

Fig. 10G is a plot of apoA-I/apoA-II weight ratios derived from data in Fig. 10B. A similar curve has been reported by Cheung and Albers (10). The minimum in the curve, equal to approximately a 1:1 apoA-I/A-II molar ratio, corresponds to the suggested location of HDL subspecies [5] and [6], which were shown in the HDL-VAP and immunoaffinity studies to constitute the bulk of the Lp(A-I with A-II) HDL fraction in the four subjects studied. As expected from the HDL-VAP and immunoaffinity studies, the A-I/A-II ratio increases in moving from the more dense to the less dense HDL[7] subspecies. This progressive yet irregular increase supports the contention that HDL[7] is heterogeneous in size, density, and composition. In the very dense apolipoprotein-rich, lipid-poor region indicated by the spikes in Fig. 10E, the apoA-I/apoA-II molar ratio decreases from ~2 in fraction 5 to ~1 in fraction 8.

DISCUSSION

The lack of any obvious change in the size and density of the three HDL fractions following their elution by mild acid conditions from the immunoaffinity chromatographic columns, as measured by computer-derived difference plots of the cholesterol profiles (Fig. 3), suggests minimal alteration in the structure of the Lp(A-I), LP(A-I with A-II), and Lp(A-I without A-II) particles compared to the corresponding particles in plasma. This suggests that there is neither significant loss of apolipoproteins or lipids from the three particles nor occurrence of particle fusion as the result of elution.

The histogram plots of the Lp(A-I without A-II) particle sizes measured from the electron micrographs from the four subjects examined (Fig. 5) clearly show a bimodal particle distribution, consistent with the gradient gel analyses (Fig. 6) indicating two major particles, HDL[4] and

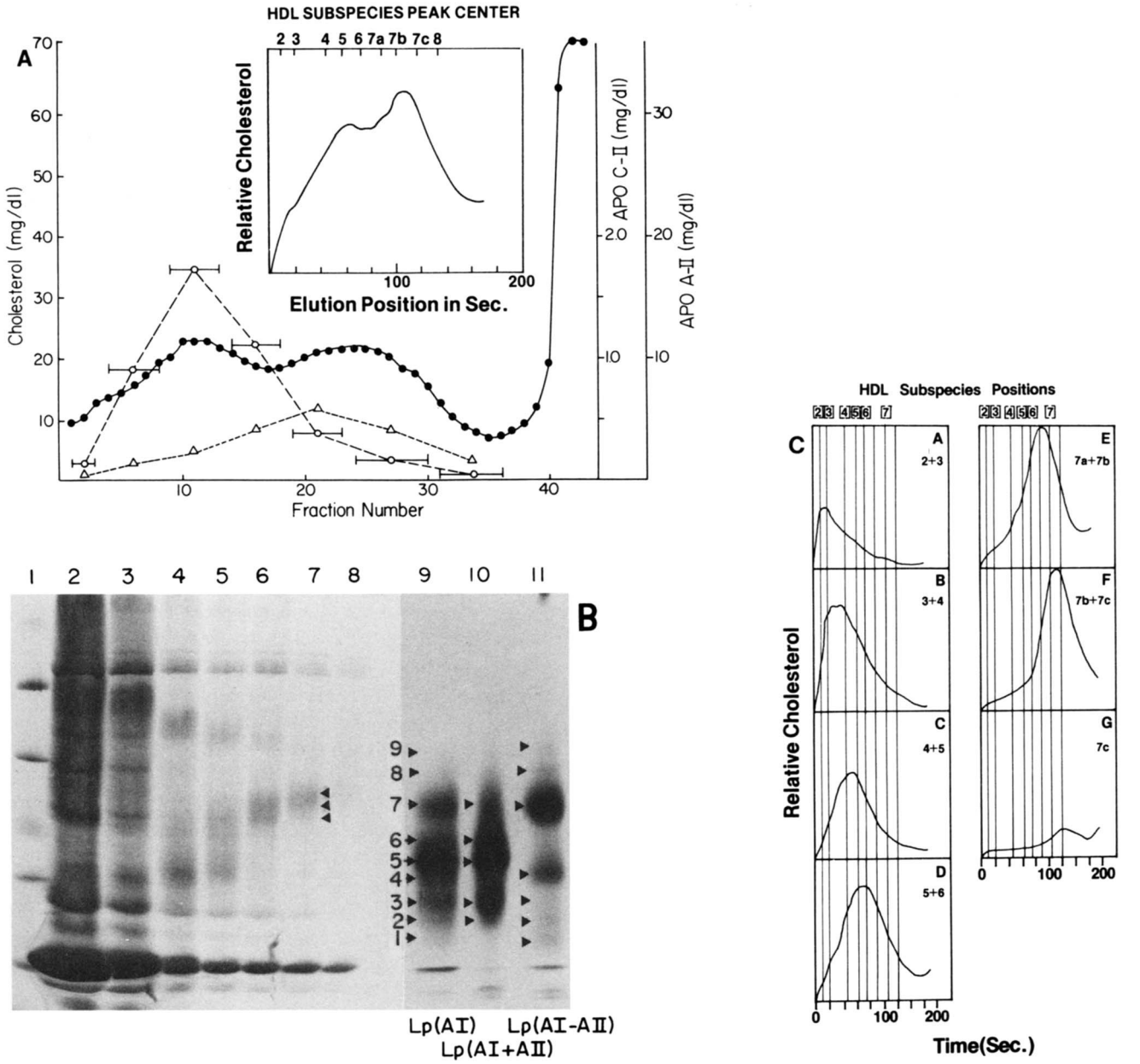

Fig. 9. A, (Insert), HDL-VAP analysis (1.5-hr spin) of whole plasma from subject M-3. The estimated peak centers for the HDL subspecies [2–8] are indicated. A, HDL-SVS fractionation (2.5-hr spin) of plasma; (●—●), total cholesterol measured by ABA-200; (○---○), apoa-II measured by radioimmunoassay; (△---△), apoC-II measured by radioimmunoassay; (⊢ ⊣), pools 1–7. B, Nondenaturing gradient gel analysis of the pools 1–7 from A stained by Coomassie blue (lanes 2–8, respectively). Lanes 9–11 are the gradient gel analyses of the different A-I-containing lipoprotein particles isolated by immunoaffinity chromatography of F-2 that are used as a marker for the HDL subspecies 1–7. The three arrow heads to the right of lane 7 denote three resolvable bands in HDL[7]. C, HDL-VAP analyses (1.5-hr spin) of pools 1–7 (A–G, respectively) from A. The probable peak centers of the HDL subspecies [2–8] are indicated on the x-axes. The predominant subspecies compositions of each pool are indicated at the upper right of the appropriate curve.

HDL[7]. With one exception, the size of the particles determined by electron microscopy and density gradient electrophoresis are comparable. The exception is that the Stokes diameter calculated from gradient gels for HDL[4], the smaller of the two particles, is 85 Å, while the mean diameter of the small particle mode in Fig. 4 is 72 Å. These observed differences are consistent with the presence of other particles in Lp(A-I without A-II), such as subspecies [1] and [2], as well as particles that are smaller than the size of our smallest protein standard and were not included in our gradient gel calculation. The HDL-VAP analysis of Lp(A-I without A-II), in all four subjects, indicates the presence of a lipoprotein peak in the region of the gradient near 10 sec.

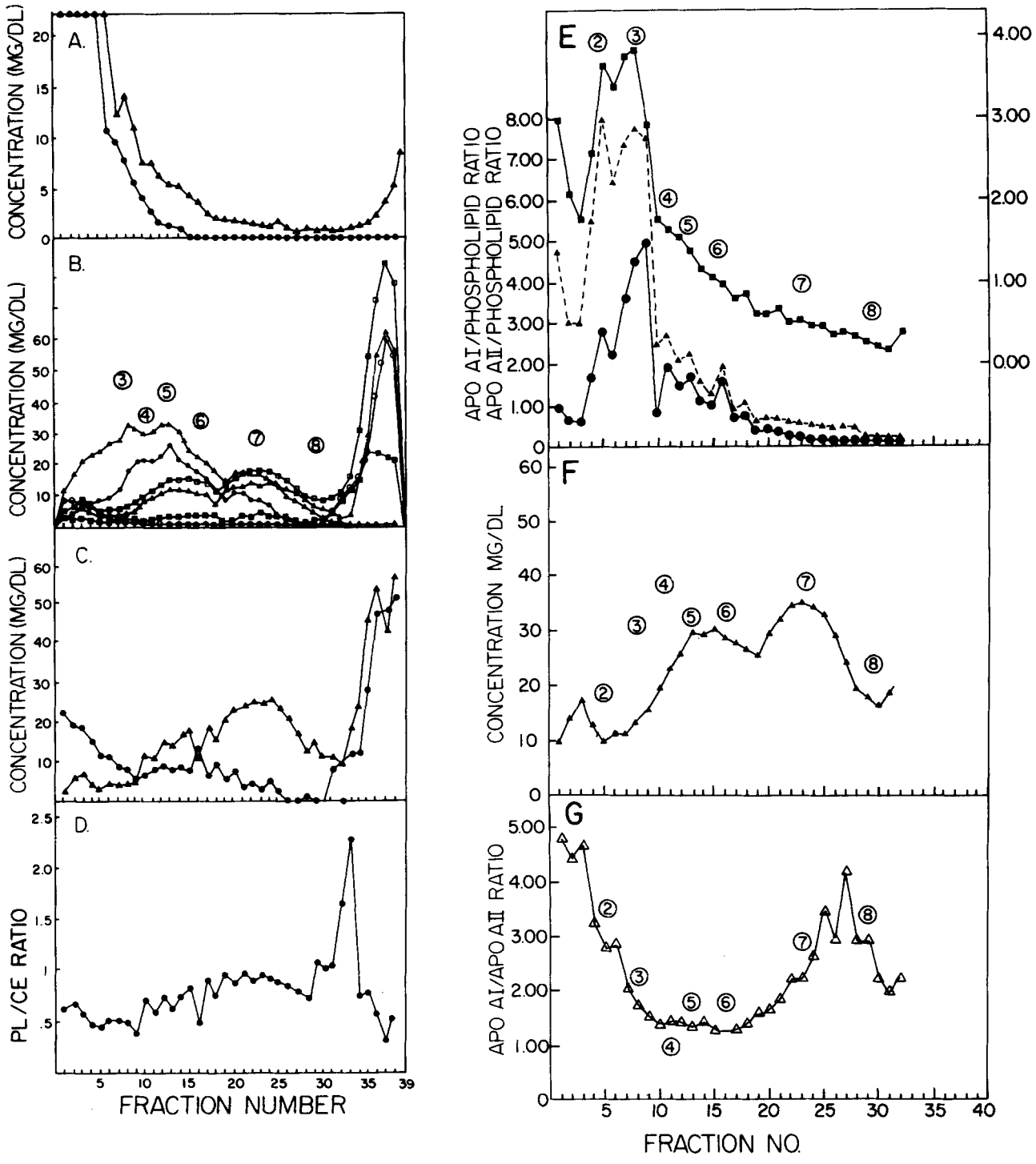

Fig. 10. Chemical analyses of HDL fractionated by HDL-SVS (5.5-hr spin). A, (△—△), albumin; (●—●), total protein measured by the Lowry procedure. B, (□—□) total cholesterol measured by the enzymatic method; (△—△), cholesteryl ester measured by the enzymatic method; (■—■), unesterified cholesterol measured by the enzymatic method; (▲—▲), apoA-I measured by radioimmunoassay; (●—●), apoA-II measured by radioimmunoassay; (○—○), apoB measured by radioimmunoassay. Cholesterol measurements had a coefficient of variation between duplicates of 4% and apolipoprotein measurements a coefficient of variation of 3%. C, (▲—▲), total phospholipid measured by phosphorus assay; (●—●), total triacylglyceride measured by the enzymatic method. Phospholipid measurements had a coefficient of variation of 8% and triglyceride measurements a coefficient of variation of 10%. D, (●—●), total phospholipid/cholesteryl ester ratio (w/w). E, Apolipoprotein to lipid weight ratios. (■—■), apoA-I/cholesteryl ester; (▲···▲), apoA-I/phospholipid; (●—●), apoA-II/phospholipid. F, Total cholesterol measured by the enzymatic method for subject in B (▲—▲). G. ApoA-I/apoA-II weight ratios derived from radioimmunoassay data in B.

It seems likely that HDL subspecies [7], [6], [5], [4], and [3] are within the size region of the subspecies defined by Blanche et al. (4) as (HDL)gge subpopulations 2b, 2a, 3a, and 3b; thus (HDL_{3a})gge contains both subspecies [4] and [5]. (HDL_{3c})gge was noted to be a minor rather inconsistently observed subspecies (4). It is likely that this subspecies corresponds to subspecies [1] and [2] as described in this report.

These results suggest that a new nomenclature for HDL subspecies is required. While we use both the broader designations Lp(A-I), Lp(A-I with A-II), and Lp(A-I without A-II) and the narrower designations HDL [1],[2],[3],[4],[5],[6],[7a],[7b],[7c],[8], and [9] for HDL subspecies in this report, an ideal nomenclature should include apolipoprotein stoichiometry, as suggested previously by Kostner and Alaupovic (1) in their lipoprotein family hypothesis. In addition, it is possible that density and/or size will have to be considered in a future nomenclature to account for any HDL particle size variation due solely to apolipoprotein conformational differences. The results of the studies reported here point to the significant limitations of the use of HDL_2 and HDL_3 fractions defined on the basis of standard sequential flotation density cuts of 1.063–1.125 and 1.125–1.21 g/ml, respectively, for studying HDL structure and metabolism.

The single vertical spin and vertical autoprofile procedures for fractionation of HDL have the advantage of extremely short spin times of 1.5 hr for the HDL-VAP and 2.5 hr for the HDL-SVS. Further, the HDL-VAP qualitatively reproduces the results obtained with immunoaffinity chromatography, gradient gel electrophoresis, and electron microscopy.

Estimated positions for HDL subspecies, as defined by gradient gel electrophoresis, have been included in the HDL-VAP analyses of Figs. 7 and 9. A discussion of the rationale for assignment of HDL subspecies to HDL-VAP curves is presented here.

Figs. 7A and 7B show a well-defined shoulder in the whole plasma curves at approximately 10–20 sec. Additional evidence for a peak at 10–20 sec is seen in Fig. 9C. We have designated this fraction HDL[2,3]. A speculative possibility is that this fraction could represent the apoA-I-rich, lipid-poor HDL subspecies indicated by Fig. 10E and recently reported by Kunitake, LaSala and Kane (28).

HDL[3] seems reasonably well localized by the HDL-VAP analyses of the Lp(A-I with A-II) fractions in Fig. 7A and 7B to approximately 20 sec. This position assignment agrees with curve shoulders seen in Figs. 9A (insert), and 10C at approximately the same position. From the HDL-VAP curves for Lp(A-I without A-II) in Figs. 7A and 7B, one can surmise that HDL[4] is located somewhere between 40 and 50 secs.

It is known from the gradient gel electrophoresis studies that Lp(A-I with A-II) contains both HDL[5] and HDL [6]. The HDL-VAP curves for Lp(A-I with A-II) in Fig. 7 indicate that the curve from F-1 is more prominent in the 60-sec position, while the curve for M-1 is more prominent in the 75-sec region. This observation is compatible with the presence of a notch at 75 sec in the HDL-VAP analyses of whole plasma from F-1, a notch not present on the corresponding analysis for M-1. The gradient gel analyses shown in Fig. 6 suggest a higher HDL[6]/HDL[5] ratio in subject M-1 than in subject F-1, which lends some support to presumptive positions for HDL[5] and HDL[6] in the HDL-VAP curves at 60 and 75 sec, respectively. Peaks at 60 and 75 sec are also noted in Fig. 9A (insert).

Evidence for a minimum of three separate subspecies in the HDL[7] region has been derived from the results of Figs. 8, 9, and 10 of this report. Additional evidence for these subspecies that we have designated HDL[7a], [7b], and [7c] derives from the HDL-VAP analyses of Lp(A-I without A-II) from subject F-1 shown in Fig. 7A; the HDL[7] region of this curve shows three obvious but closely spaced shoulders at 90, 100, and 120 sec. Fig. 9A (insert) supports similar locations for HDL[7a] and [7b], as does Fig. 10C for HDL[7a] and [7c].

From the above considerations we have arrived at HDL-VAP consensus positions for HDL[2],[3],[4], [5],[6],[7a],[7b], and [7c], at 10 sec, 20 sec, 42 sec, 61 sec, 75 sec, 90 sec, 103 sec, and 120 sec, respectively.

Together, HDL-VAP, gradient gel analysis, and electron microscopy allow a tentative assignment of HDL subspecies positions to the preparative HDL-SVS fractionations shown in Figs. 8 and 10. With the exception of HDL[7], assignment of more exact positions for the HDL subspecies must await isolation of subspecies [3–6] and HDL-SVS analysis on the isolated peaks.

The correspondence between the HDL-VAP curves for Lp(A-I without A-II) in Fig. 7 and the curves for apoC-II in Fig. 8 raises the possibility that apoC-II may be able to substitute for apoA-II. From this one might speculate that substitution of apoC-II for apoA-II is at least partially involved in the structural differentiation of Lp(A-I with A-II) particles from Lp(A-I without A-II) particles. The presence of variable amounts of apoA-II in HDL[7] is consistent with this possibility.

As shown in **Table 3,** the difference in surface area of HDL[4] compared to HDL[3], HDL[5] compared to HDL[4], and HDL[6] compared to HDL[5] averages 2600 ± 300 Å^2, the difference in surface area of HDL[7b] compared to HDL[7a] and HDL[7c] compared to HDL[7b] averages 3400 ± 100 Å^2, while the difference in surface area of HDL[7a] compared to HDL[6] is 5600 Å^2. This is reminiscent of the results we previously noted for apolipoprotein A-I/DMPC recombinants (29), in which incremental changes in discoidal diameter between several discrete recombinant particles containing two apoA-I molecules per disc (R-2) on the one hand and be-

TABLE 3. Summary of physical and chemical properties of HDL subspecies

HDL Subspecies	Diameter	Increase in Surface Area[a]	Average Increase	Chol/A-I Molar Ratio	PL/A-I Molar Ratio	Apolipoprotein/A-I Molar Ratio	
						A-II	C-II
	Å	Å^2					
3	81			13	5	0.52	0.01
4	85	2100		11	15	0.0	0.01
5	90	2700	2567	23	19	0.75	0.02
6	95	2900		29	30	0.95	0.05
7a	104	5627		33	57	0.71	0.09
7b	109	3346	3424	38	72	0.44	0.15
7c	114	3502		83	91	0.42	0.27
8	121	5900					

[a]Over that of the preceding smaller subspecies. For example, an HDL[4] particle has a surface area 2100 Å^2 greater than an HDL[3] particle.

tween several discrete recombinant particles containing three apoA-I molecules per disc (R-3) on the other hand were quantized at ~13 Å, while the difference between the diameters of the largest R-2 particle and the smallest R-3 particle was almost twice as large at 22 Å. Our interpretation of these results was that the 13 Å-quantized changes in discoidal diameter represented quantized conformational changes in amphipathic helical regions of apoA-I, while the larger 22 Å change represented the addition or subtraction of a third molecule of apoA-I. We would like to suggest here that similar mechanisms involving changes in apolipoprotein A-I conformation and stoichiometry may be involved in the structural, and probably functional, transitions between HDL subspecies.

Given known HDL lipoprotein subspecies compositions and particle diameters, there are two ways to derive apolipoprotein stoichiometry for a given subspecies: surface area calculations and volume calculations. The particle diameters from Table 2 are known to a reasonable degree of precision; the compositional data in Table 3, however, is imprecise, primarily because of overlapping subspecies in the gradients. Nevertheless, even though the results are necessarily only approximate, we thought it useful to make calculations of apolipoprotein stoichiometry.

From Table 3 one can calculate that the average incremental change in the number of phospholipid molecules per apoA-I, excluding the change between HDL[6] and HDL[7a], is 11.8. At one, two, three, or four apoA-I molecules per HDL subspecies particle, this equals 600–1100 Å^2, 1300–2100 Å^2, 1900–3200 Å^2, or 2600–4200 Å^2 increases in surface area, assuming an allowable mean surface area range of 54–87 Å^2 per phospholipid molecule (30). We previously suggested that the quantized changes in amphipathic helical regions of apoA-I represented ~two to three amphipathic helixes (29). On the basis of helical hydrophobic moment calculations (31), the central region of tandem repetitive amphipathic helical repeats in apoA-I contains a region of three helical domains with relatively low helical hydrophobic moments compared to their neighbors (M. C. Phillips, personal communication). Three amphipathic helical segments would occupy an area of ~810–1140 Å^2 (18 residues × 1.5 Å/residue × 10–14 Å helical cross-sectional diameter × 3); two amphipathic helical segments would occupy ~540–760 Å^2.

From these calculations, a table of predicted surface area changes for particles containing one to four apoA-I molecules plus associated phospholipid per particle has been constructed **(Table 4).** The average difference in

TABLE 4. HDL subspecies surface area calculations

Moles ApoA-I per Mole Subspecies	Surface Area Change Assuming Three Amphipathic Helixes per Hinged Domain (Includes Associated PL)	Surface Area Change Assuming Two Amphipathic Helixes per Hinged Domain (Includes Associated PL)
	Å^2	Å^2
1	1500–2200	1200–1800
2	2100–3200[a]	1800–2900[a]
3	2800–4300[b]	2500–3900[a,b]
4	3400–5300[b]	3100–5000[b]

[a]Surface area change calculated for HDL 3–6 (2600 Å^2) falls within this range.
[b]Surface area change calculated for HDL 7a–7c (3400 Å^2) falls within this range.

surface area for HDL subspecies 3–6 (2600 Å^2) corresponds closest to the surface area changes predicted for two apoA-I molecules per particle, although it does fall within the range predicted for three apoA-I molecules per particle and two amphipathic helixes per hinged domain; the average difference for HDL subspecies 7a–7c (3400 Å^2) corresponds closest to the surface area changes predicted for three apoA-I molecules per particle, although it does fall within the range predicted for four apoA-I molecules per particle (Table 4).

Because a recent report utilizing chemical crosslinking by Nichols et al. (32) suggests that the particles corresponding to HDL subspecies 5 and 6 may contain three apoA-I molecules per particle and those corresponding to HDL subspecies 7a–7c may contain four apoA-I molecules per particle, the question of apoA-I stoichiometry was pursued further. HDL subspecies volumes (and corresponding diameters) can be calculated for a number of possible apolipoprotein and lipid stoichiometries (and compared to measured diameters) when the molecular volumes of the individual components are available. Molecular volumes for the lipid components of HDL, phospholipid (1270 Å^3), cholesteryl ester (1090 Å^3), cholesterol (600 Å^3), and triglycerides (1600 Å^3), are known with a fair degree of precision (33). As a first approximation, the molecular volumes for apoA-I and apoA-II were calculated to be 87,114 Å^3 and 53,983 Å^3, respectively, by the following procedure. *a*) The Stokes radius of apoA-I, 27.5 Å, is equal to a sphere of volume 87,114 Å^3. *b*) The Stokes radius of serum albumin, 36.5 Å, is equal to a sphere of volume 203,689 Å^3. *c*) Given a molecular weight of 28,016 and 66,200 for apoA-I and serum albumin, respectively, specific molecular volumes (V_m) of 3.109 Å^3/Dalton and 3.077 Å^3/Dalton were calculated for apoA-I and albumin, respectively. *d*) Based on calculations of V_m for a large number of proteins from crystallographic data, the value of ~3.1 Å^3/Dalton falls within the known frequency distribution for proteins (34). A V_m of 3.1 Å^3/Dalton was therefore used to calculate a molecular volume of 53,983 Å^3 for apoA-II from its molecular weight of 17,414.

Using the above molecular volumes, the HDL subspecies volumes (and corresponding diameters) were calculated for a number of possible stoichiometries **(Table 5).** For HDL[5], HDL[6], and HDL[7b] the best fit in every case to the known volumes and diameters from the nondenaturing gradient gel analyses (Table 2) was to models assuming two apoA-I molecules per HDL[5] and HDL[6] particle and three apoA-I molecules per HDL[7b] particle.

On the other hand, a V_m of 3.1 Å^3/Dalton falls within the more loosely packed end of the frequency distribution of V_m for proteins (34). Such a large V_m is likely for apoA-I and apoA-II in solution but probably is too large for these apolipoproteins associated with lipid. When a median V_m of 2.25 Å^3/Dalton is used in calculations, none of the stoichiometries listed in Table 5 give close fits to the known diameters of the subspecies HDL[5], HDL[6], and HDL[7b]. However, given a stoichiometry of three apoA-I per particle and a diameter of 90 Å, one can calculate a V_m for the apoA-I and apoA-II of HDL[5] of 1.91 Å^3/Dalton; this value falls within the most densely packed end of the V_m distribution (34). Using this V_m and assuming a stoichiometry of four apoA-I per particle, a diameter for HDL[7b] of 108 Å is calculated, which compares well to the measured diameter of 109 Å. The

TABLE 5. HDL subspecies volume calculations

Subspecies	Source of Data[a]	A-I	A-II	PL	CE	C	TG	Volume[b]	Stokes Diameter
		moles/mole subspecies						*Å* ^{3}	*Å*
HDL[5]	GGE							3.82×10^5	90
HDL[5]	A	2	2	38	19	5	6	3.67×10^5	89
HDL[5]	B	3	1	93	44	11	9	5.03×10^5	99
HDL[5]	C	2	1	62	29	7	6	3.53×10^5	88
HDL[5]	C	2	2	62	29	7	6	4.07×10^5	92
HDL[6]	GGE							4.49×10^5	95
HDL[6]	A	2	2	60	46	12	9	4.31×10^5	94
HDL[7b]	GGE							6.78×10^5	109
HDL[7b]	A	3	1	216	91	23	14	7.32×10^5	112
HDL[7b]	B	4	1	189	109	52	18	8.31×10^5	116
HDL[7b]	D	3	1	142	82	39	14	6.31×10^5	106

[a] A, Table 2; B, Eisenberg (35); C, lipids from Eisenberg (35) assuming two apoA-I molecules per particle (lipids equal to ⅔ of Eisenberg values); D, lipids from Eisenberg (35) assuming three apoA-I molecules per particle (lipids equal to ¾ of Eisenberg values); GGE nondenaturing gradient gel electrophoresis.

[b] Calculated using the following molecular volumes: apoA-I, 87,114 Å^3 (calculated from Stokes diameter of 27.5 Å); apoA-II, 53,983 Å^3 (calculated assuming specific molecular volume of 3.1 Å^3/Dalton); phospholipid, 1,270 Å^3; cholesteryl ester, 1,090 Å^3; cholesterol, 600 Å^3; and triacylglyceride, 1,600 Å^3 (33).

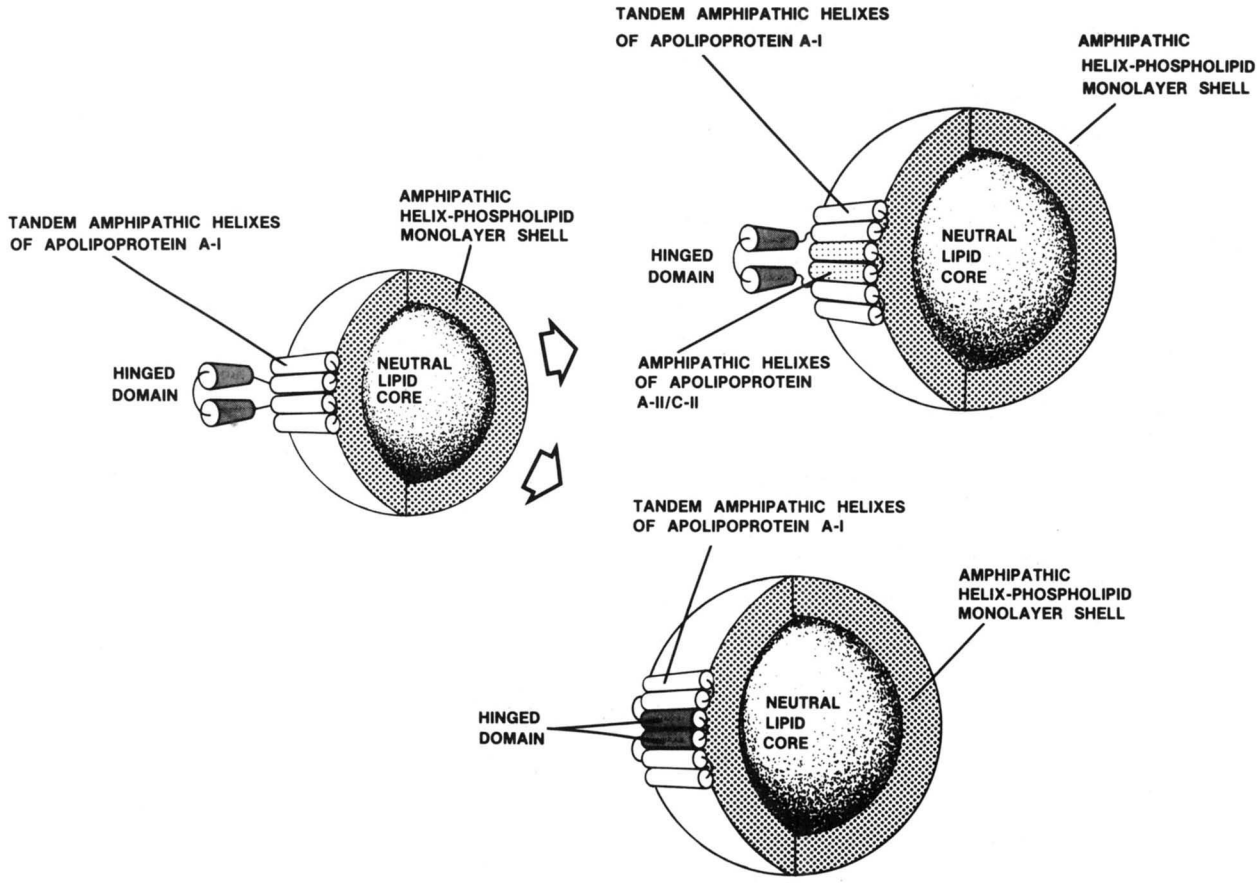

Fig. 11. Schematic illustration of the hinged domain hypothesis.

calculated diameter of 108 Å increases to 111 Å if one assumes the presence of one molecule each of apoC-I, C-II, and C-III per HDL[7b] particle.

Based on the calculations of Tables 4 and 5 and the additional data presented in this report, we propose the following speculative model (diagrammatically illustrated in **Fig. 11)** for the structure of HDL subspecies. *a*) HDL subspecies [3],[4],[5], and [6] contain either two or three apoA-I molecules per particle and HDL subspecies [7a], [7b], and [7c] contain either three or four apoA-I molecules per particle. *b*) The incremental changes in surface area between adjacent subspecies in the two different apoA-I stoichiometry classes are due to a single quantized conformation change in apoA-I and/or the addition of one molecule of apoA-II. *c*) The single conformational change in apoA-I produces a hinge-like change, and thus a change in HDL surface-association, of a quantized number of amphipathic helical domains of apoA-I. *d*) The apoA-I hinged domain is approximately equivalent in its effect on HDL surface area to that of a single apoA-II molecule. *e*) The defect created by removal of the quantized unit of amphipathic helixes of apoA-I from the HDL surface, the hinged domain, can be filled by a single apoA-II molecule. *f*) ApoC-II (and perhaps other apolipoproteins) can substitute for apoA-II. This putative substitution is concentrated in, but not limited to, the HDL[7] and HDL[4] subspecies.

Considering the possibility that there may be apolipoprotein heterogeneity within each of the HDL subspecies defined in this paper, the number of distinct HDL subspecies may be considerably greater than eleven. An important goal of our future research will be to further define the stoichiometry of HDL subspecies. It is hoped we can simultaneously establish a unifying concept to explain the structural complexity of these lipoproteins; the hinged-domain hypothesis is the initial working model. Structural knowledge should prove useful in attempting to understand the roles of the multitude of HDL particles in lipoprotein metabolism and atherogenesis.

We are indebted to Ms. Joan Benderson and Anitra Wolf for their expert technical assistance, to Retha Donald for typing the manuscript and to Dr. John Brunzell for his helpful suggestions. This work was supported in part by NIH grants HL-28388 and

HL-34343 (JPS), HL-30086 (M. C. C. and J. J. A.), and by the Council for Tobacco Research-USA. Inc. (J. J. A.).

Manuscript received 10 December 1985, in revised form 2 July 1986, and in re-revised form 23 March 1987.

REFERENCES

1. Kostner, G., and P. Alaupovic. 1972. Studies of the composition and structure of plasma lipoprotein. Separation and quantification of the lipoprotein families occurring in the high density lipoproteins of human plasma. *Biochemistry.* **11:** 3419–3428.
2. Fielding, P. E., and C. J. Fielding. 1980. A cholesteryl ester transfer complex in human plasma. *Proc. Natl. Acad. Sci. USA.* **77:** 3327–3330.
3. Weisgraber, K. H., and R. W. Mahley. 1980. Subfractionation of human high density lipoproteins by heparin-Sepharose affinity chromatography. *J. Lipid Res.* **21:** 316–325.
4. Blanche, P. J., E. L. Gong, T. M. Forte, and A. V. Nichols. 1981. Characterization of human high density lipoproteins by gradient gel electrophoresis. *Biochim. Biophys. Acta.* **665:** 408–419.
5. Schmitz, G. and G. Assmann. 1982. Isolation of human serum HDL_1 by zonal ultracentrifugation. *J. Lipid Res.* **23:** 903–910.
6. Patsch, W., G. Schonfeld, A. M. Gotto, Jr., and J. Patsch. 1980. Characterization of human high density lipoproteins by zonal ultracentrifugation. *J. Biol. Chem.* **255:** 3178–3185.
7. Scanu, A. 1985. Studies on the conformation of human high density lipoproteins HDL_3 and HDL_2. *Proc. Natl. Acad. Sci. USA.* **54:** 1699–1705.
8. Havel, R. J., H. A. Eder, and J. H. Bragdon. 1955. The distribution and chemical composition of ultracentrifugally separated lipoproteins in human serum. *J. Clin. Invest.* **34:** 1345–1353.
9. Kraus, R. M., F. T. Lindgren, and R. W. Ray. 1980. Interrelationships among subgroups of serum lipoproteins in normal human subjects. *Clin. Chim. Acta.* **104:** 275–290.
10. Cheung, M. C., and J. J. Albers. 1982. Distribution of high density lipoprotein particles with different apoprotein composition: particles with A-I and A-II and particles with A-I but no A-II. *J. Lipid Res.* **23:** 747–753.
11. Patsch, J. R. 1982. Metabolic aspects of subfractions of serum lipoproteins. *In* Metabolic Risk Factors in Ischemic Cardiovascular Disease. L. A. Carlson and B. Pernow, editors. Raven Press, New York. 123–131.
12. Cheung, M. C., and J. J. Albers. 1984. Characterization of lipoprotein particles isolated by immunoaffinity chromatography. Particles containing A-I and A-II and particles containing A-I but no A-II. *J. Biol. Chem.* **259:** 12201–12209.
13. Chung, B. H., T. Wilkinson, J. C. Geer, and J. P. Segrest. 1980. Preparative and quantitative isolation of plasma lipoproteins: rapid, single discontinuous density gradient ultracentrifugation in a vertical rotor. *J. Lipid Res.* **21:** 284–291.
14. Chung, B. H., J. P. Segrest, J. T. Cone, J. Pfau, J. C. Geer, and L. A. Duncan. 1981. High resolution plasma lipoprotein cholesterol profiles by a rapid, high volume, semi-automated method. *J. Lipid Res.* **22:** 1003–1014.
15. Cone, J. T., J. P. Segrest, B. H. Chung, J. B. Ragland, S. M. Sabesin, and A. Glasscock. 1982. Computerized rapid high resolution quantitative analysis of plasma lipoproteins based upon single vertical spin centrifugation. *J. Lipid Res.* **23:** 923–935.
16. Cheung, M. C., and J. J. Albers. 1977. The measurement of apolipoprotein A-I and A-II levels in men and women by immunoassay. *J. Clin. Invest.* **60:** 43–50.
17. Albers, J. J., P. W. Wahl, V. G. Cabana, W. R. Hazzard, and J. J. Hoover. 1976. Quantification of apolipoprotein A-I of human plasma high density lipoprotein. *Metabolism.* **25:** 633–644.
18. Doumas, B. T., W. A. Watson, and H. G. Biggs. 1971. Albumin standards for the measurement of serum albumin with bromcresol green. *Clin. Chim. Acta.* **31:** 87–96.
19. Lowry, O. H., N. J. Rosebrough, A. L. Farr, and R. J. Randall. 1981. Protein measurement with the Folin phenol reagent. *J. Biol. Chem.* **193:** 265–275.
20. Jackson, R. L., B. H. Chung, L. C. Smith, and O. D. Taunton. 1977. Physical chemical and immunochemical characterization of a lipoprotein lipase activator protein from pig palsma very low density lipoproteins. *Biochim. Biophys. Acta.* **490:** 385–394.
21. Kashyap, H. L., L. S. Srivastava, C. Y. Chen, G. Perisutti, M. Campbell, R. F. Lutmer, and C. J. Glueck. 1977. Radioimmunoassay of human apolipoprotein C-II. A study in normal and hypertriglyceridemic subjects. *J. Clin. Invest.* **60:** 171–180.
22. Albers, J. J., J. L. Adolphson, and C. H. Chen. 1981. Radioimmunoassay of human plasma lecithin:cholesterol acyltransferase. *J. Clin. Invest.* **67:** 141–148.
23. Steward, J. 1980. Colorimetric determination of phospholipids with ammonium ferrothiocyanate. *Anal. Biochem.* **104:** 10–14.
24. Bucolo, G., and H. David. 1973. Quantitative determination of serum triglycerides by the use of enzymes. *Clin. Chem.* **19:** 476–482.
25. Chung, B. H., G. M. Anantharamaiah, G. C. Brouillette, T. Nishida, and J. P. Segrest. 1985. Studies of synthetic peptide analogs of the amphipathic helix: correlation of structure with function. *J. Biol. Chem.* **260:** 10256–10262.
26. Segrest, J. P., C. G. Brouillette, B. H. Chung, C. F. Schmidt, A. Gawish, and G. M. Anantharamaiah. 1985. Structure–function studies of synthetic peptide analogs of the amphipathic helix. *Arteriosclerosis.* **5:** 546a.
27. Anantharamaiah, G. M., C. G. Brouillette, B. H. Chung, C. F. Schmidt, A. Gawish, and J. P. Segrest. 1985. Synthetic peptide analogs of apolipoproteins. *In* Peptides. Deber, C. F., V. J. Hruby, and K. D. Kopple, editors. Pierce Chemical Co., Rockford, IL. 903–907.
28. Kunitake, S. T., K. J. LaSala, and J. P. Kane. 1985. Apolipoprotein A-I-containing lipoproteins with pre-beta electrophoretic mobility. *J. Lipid Res.* **26:** 549–555.
29. Brouillette, C. G., J. L. Jones, T. C. Ng, H. Kercret, B. H. Chung and J. P. Segrest. 1984. Structural studies of apolipoprotein A-I/phosphatidylcholine recombinants by high-field proton NMR, nondenaturing gradient gel electrophoresis, and electron microscopy. *Biochemistry.* **23:** 359–367.
30. Brouillette, C. G., J. P. Segrest, T. C. Ng, and J. L. Jones. 1982. Minimal size phosphatidylcholine vesicles: effects of radius of curvature on head group packing and conformation. *Biochemistry.* **21:** 4569–4575.
31. Eisenberg, D., R. M. Weiss, and T. C. Terwilliger. 1982. The helical hydrophobic moment: a measure of the amphiphilicity of a helix. *Nature.* **299:** 371–374.

32. Nichols, A. V., M. C. Cheung, P. Blanche, and E. Gong. 1985. Relevance of model transformation studies to origins of HDL subpopulations. *Arteriosclerosis.* **5:** 545a.
33. Edelstein, C., F. J. Kezdy, A. M. Scanu, and B. W. Shen. 1979. Apolipoproteins and the structural organization of plasma lipoproteins: human plasma high density lipoprotein-3. *J. Lipid Res.* **20:** 143–153.
34. Mathews, B. W. 1968. Solvent content of protein crystals. *J. Mol. Biol.* **33:** 491–497.
35. Eisenberg, S. 1984. High density lipoprotein metabolism. *J. Lipid Res.* **25:** 1017–1058.